analytical chemistry

Article

pubs.acs.org/ac

Toward Complete Miniaturisation of Flow Injection Analysis Systems: Microfluidic Enhancement of Chemiluminescent Detection

Ana M. Gracioso Martins,[†] Nick R. Glass,[‡,§] Sally Harrison,[†] Amgad R. Rezk,[‡] Nichola A. Porter,[†] Peter D. Carpenter,[†] Johan Du Plessis,[†] James R. Friend,[‡] and Leslie Y. Yeo*[,‡]

[†]Centre for Environmental Science and Remediation, School of Applied Sciences, RMIT University, Melbourne, Victoria 3000, Australia

[‡]Micro/Nanophysics Research Laboratory, RMIT University, Melbourne, Victoria 3000, Australia

[§]Monash University, Clayton, Victoria 3800, Australia

ABSTRACT: Conventional flow injection systems for aquatic environmental analysis typically comprise large laboratory benchscale equipment, which place considerable constraints for portable field use. Here, we demonstrate the use of an integrated acoustically driven microfluidic mixing scheme to enhance detection of a chemiluminescent species tris(2,2′-bipyridyl)dichlororuthenium(II) hexahydrate—a common chemiluminescent reagent widely used for the analysis of a wide range of compounds such as illicit drugs, pharmaceuticals, and pesticides—such that rapid in-line quantification can be carried out with sufficient on-chip sensitivity. Specifically, we employ surface acoustic waves (SAWs) to drive intense chaotic streaming within a 100 μL chamber cast in polydimethoxylsiloxane (PDMS) atop a microfluidic chip consisting of a single crystal piezoelectric material. By optimizing the power, duration, and orientation of the SAW input, we show that the mixing intensity of the sample and reagent fed into the chamber can be increased by one to two orders of magnitude, leading to a similar enhancement in the detection sensitivity of the chemiluminescent species and thus achieving a theoretical limit of detection of 0.02 ppb (0.2 nM) of L-proline—a decade improvement over the industry gold-standard and two orders of magnitude more sensitive than that achievable with conventional systems—simply using a portable photodetector and without requiring sample preconcentration. This on-chip microfluidic mixing strategy, together with the integrated miniature photodetector and the possibility for chip-scale microfluidic actuation, then alludes to the attractive possibility of a completely miniaturized platform for portable field-use microanalytical systems.

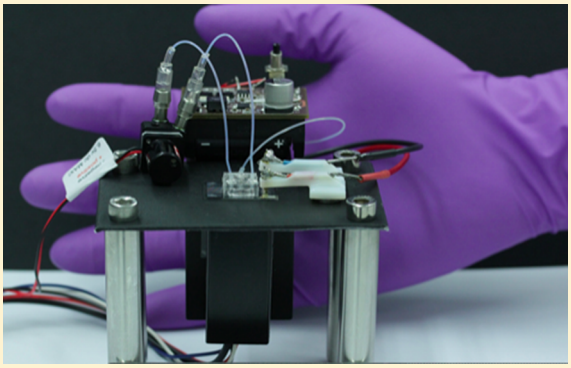

Flow injection analysis (FIA) is a versatile analytical technique widely used for the analysis of chemical species in liquid phase,[1−5] wherein species are quantified as a function of the signal produced by a detectable change in physical property (pH, conductivity, electrode potential, wavelength, light absorption, or emission) at any given point of a reaction coordinate in a dynamic flow system.[2,6] This flexibility makes FIA a powerful method for liquid phase chemical quantification, especially for the analysis of environmental, food, and biological samples. Nevertheless, the requirement of laboratory benchscale equipment for sample preparation (usually a multistep procedure) and injection, reaction as well as detection in conventional FIA typically prohibit miniaturization of these systems to exploit the advantages of low reagent consumption and short analysis times, as well as portable field use—the latter desirable for applications such as on-site water testing of pollutants and water quality monitoring, which should ideally be performed in situ[7] at a fixed point or on board sampling vessels.[8] Even when portability is claimed, the reported FIA systems are still relatively large, cumbersome and heavy (see, for example, ref 8.) Moreover, the sub-ppb detection sensitivity necessary for water monitoring and testing[9] often necessitates additional equipment for sample preconcentration in these systems, which further limits options for their portability.[6]

In this work, we attempt to design and test a microfluidic FIA platform that addresses these limitations in order to enable in situ point source microanalyses or continuous field monitoring without requiring sample preconcentration. Advances in detection technology have since significantly improved detector sensitivity, which, together with optimized reaction kinetics, has facilitated the quantification of a range of previously undetectable compounds. For example, the use of photochemical oxidative processes, derivatization, immunoassays,[10] fluorescent labels,[6,11,12] and even the immobilization of reactants or substrates onto newly designed materials[13,14] has vastly extended the repertoire of FIA as a flexible and sensitive microanalytical technique. For example, FIA-Chemiluminescence (FIA-CL)[15] and FIA-Fluorescence (FIA-FL)[16] offer the

Received: August 1, 2014
Accepted: October 2, 2014
Published: October 2, 2014

   dx.doi.org/10.1021/ac502878p | *Anal. Chem.* 2014, 86, 10812−10819

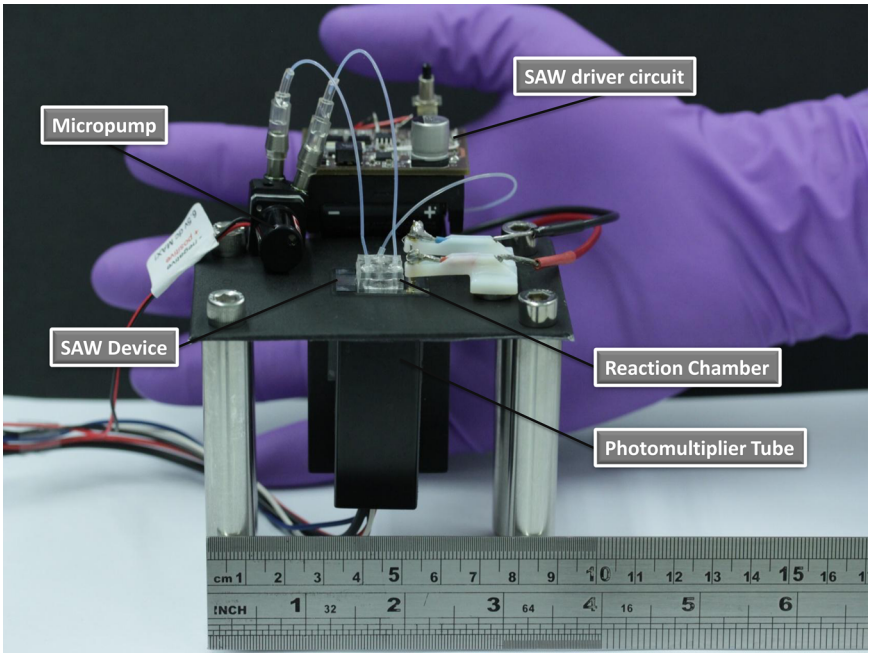

Figure 1. Image of the proposed portable FIA system which includes a micropump, the SAW chip powered by a miniature driver circuit that includes a signal generator and amplifier, the PDMS reaction chamber bonded to the chip and a portable photodetector, showing the possibility for complete integration and portability for field use. The total weight of the entire system is approximately 130 g.

possibility for limits of quantification that are comparable to those of other sensitive conventional analytical techniques such as CE, LC-MS, and GC-MS.[17−19] Further, chemiluminescent reagents display a high degree of selectivity[17] in their reaction with chemiluminogenic compounds, emitting distinct light wavelengths that can be captured with highly sensitive detectors such as photomultiplier tubes (PMTs), charge coupled devices (CCDs), or complementary metal-oxide semiconductor (CMOS) cameras,[20] whose advances have enabled miniaturization into portable hand-held systems.

Nevertheless, the ability to completely miniaturize the FIA detection platform cannot be achieved merely by incorporating these portable sensors, especially given the compromise in detection sensitivity with scale down in size. As such, the kinetics of the reaction must be taken into account in the design of these systems in addition to favorable stereochemical conditions. Given the fast chemiluminescent reaction time scales, the process is typically diffusion-limited[21] due to the absence of turbulent mixing vortices in the typical low Reynolds number laminar flow conditions of a FIA system, and thus micromixing is an important consideration not only to increase reaction yield (in this case, the intensity of the chemiluminescent signal) and hence allow lower limits of detection with a given sensor, but also to attain sufficiently short residence times that, in turn, facilitate scale down in the dimensions of the reaction chamber. In view of their relative simplicity, passive sample-reagent mixing strategies, such as the incorporation of serpentine channels and flow obstructions, for example, have therefore been adopted in many FIA-CL platforms to increase the rate of reaction despite their lower mixing efficiencies,[22−24] longer residence times, larger associated pressure drops and fabrication complexities compared to their active counterparts. This has primarily been due to the lack of a low cost and efficient active micromixing scheme that can be easily integrated to date, especially if portability is desired.

Here, we demonstrate that the use of acoustics to drive active micromixing of any chemiluminogenic compound is able to enhance the mixing efficiency to a sufficient extent that limits of detection superior to that using both conventional benchscale FIA instrumentation as well as chemiluminescent microanalyses[25−27] can be achieved with a portable PMT integrated into a microfluidic chamber. More specifically, we exploit the use of surface acoustic waves (SAWs)—nanometre amplitude high frequency (MHz order) electromechanical waves that propagate on the surface of a piezoelectric substrate—which has recently been shown not just as a powerful tool for microscale fluid manipulation[28−30] but also one that can efficiently be driven using a battery-powered portable hand-held circuit.[31] While *batch* chaotic micromixing via SAW-generated acoustic streaming[32,33] has been demonstrated in a sessile drop,[34−39] microchamber,[40,41] microchannel,[42] microdisc,[43] and in paper,[44] the work reported here presents the first instance of a *continuous flow* micromixing strategy in addition to complete on-chip integration with a portable photodetection scheme; unlike batch systems, the residence time of the sample and reagent in the mixing chamber, which is a function of the liquid flow rate into the chamber, is an additional system consideration since it imposes a constraint on the mixing time and hence the mixing efficiency. Together with the ability to incorporate integrated chip-scale SAW continuous flow micropumps,[45] this on-chip microfluidic mixing strategy and integrated miniature photodetector therefore constitutes a completely miniaturized platform for portable field-use miniaturized FIA systems (Figure 1) that is able to improve current industry standard limits of detection even without the need for sample preconcentration.

MATERIALS AND METHODS

Materials. Tris(2,2′-bipyridyl)dichlororuthenium(II) hexahydrate ($[Ru(bipy)_3]^{2+}$) is a chemiluminescent reagent that has been widely described in the literature and utilized for the

dx.doi.org/10.1021/ac502878p | *Anal. Chem.* 2014, 86, 10812−10819

analysis of various classes of compounds such as amines, amino acids, organic acids, illicit drugs, pharmaceuticals, and pesticides.[46] Due to its wide applicability,[52] $[Ru(bipy)_3]^{2+}$ is thus the reagent of choice in this study, whose chemiluminescent reaction can be summarized by the following:

$$Ru(bipy)_3^{2+} \xrightarrow{\text{(oxidation)}} Ru(bipy)_3^{3+}$$

$$Ru(bipy)_3^{3+} + \text{Analyte} \xrightarrow{\text{(reduction)}} [Ru(bipy)_3^{2+}]^*, \text{ and}$$

$$[Ru(bipy)_3^{2+}]^* \rightarrow Ru(bipy)_3^{2+} + [Ru^{3+}(bipy)^-(bipy)_2]^{2+} + h\nu$$

In general, the $[Ru(bipy)_3]^{2+}$ species is oxidized by a catalyst into its chemiluminogenic form tris(2,2′-bipyridyl)-dichlororuthenium(III) hexahydrate ($[Ru(bipy)_3]^{3+}$). The reaction of $[Ru(bipy)_3]^{3+}$ with an electron-rich analyte then gives rise to the excited-state $[Ru(bipy)_3^{2+}]^*$, which subsequently relaxes back to its ground-state $[Ru(bipy)_3]^{2+}$ by emitting light in the form of photon energy $h\nu$, while also forming the byproduct $[Ru^{3+}(bipy)^-(bipy)_2]^{2+}$.[52] The amount of light emitted by the chemiluminescent reaction is, fundamentally, a function of the analyte concentration under optimized reaction conditions as it is the direct result of the reduction of $[Ru(bipy)_3]^{3+}$ to $[Ru(bipy)_3]^{2+}$ and $[Ru^{3+}(bipy)^-(bipy)_2]^{2+}$ by the analyte.[46]

Proline—a uniquely structured α-amino-acid featuring a secondary amine group which readily reacts with $[Ru(bipy)_3]^{3+}$—is employed as our analyte of choice given that it is widely used in similar chemiluminescent detection studies[47−51] and since numerous microanalytical chemiluminescence methods have been developed to target it for the determination of nitrogen content in amino-acid-rich matter such as foods, animal tissues, and other forms of organic matter;[25−27,46,53] other chemiluminescent reagents with similar applications are luminol, diaryloxalates and potassium permanganate.[54]

Specifically, L-proline (analytical grade; Sigma-Aldrich Pty. Ltd., Castle Hill, NSW, Australia) standards were prepared in 50.0 mM (w/w) sodium tetraborate buffer (analytical grade, Ajax Finechem; Thermo Fisher Scientific Pty. Ltd., North Ryde, NSW, Australia), adjusted to pH 9.0 using hydrochloric acid (analytical grade, Ajax Finechem; Thermo Fisher Scientific Pty. Ltd., North Ryde, NSW, Australia). 1.0 mM $[Ru(bipy)_3]^{2+}$ (analytical grade, Sigma-Aldrich Pty. Ltd., Castle Hill, NSW, Australia) was prepared in 20.0 mM sulfuric acid and oxidized to $[Ru(bipy)_3]^{3+}$ using 1.0 g of lead dioxide powder per 100 mL aliquot (analytical grade, Merck Pty. Ltd., Kilsyth, VIC, Australia) and filtered in-line using a 0.45 μm Teflon microfilter (Labquip Ltd., Dublin, Ireland).

Device Fabrication. The SAW device was designed with a simple unweighted interdigital electrode described elsewhere,[29] with 20 electrode finger pairs to operate between 19.6 and 21.5 MHz on single crystal lithium niobate in a 127.68° Y-rotated, X-propagating cut (Roditi International Corp., London, U.K.), fabricated using lift-off photolithography. Briefly, double-sided polished lithium niobate wafers were piranha-cleaned (3:1 H_2SO_4/H_2O_2) for 20 min. The wafers were then rinsed with water and isopropanol and subsequently dried with nitrogen. AZ4562 photoresist (MicroChemicals GmbH, Ulm, Germany) was spin coated onto the wafers to a thickness of approximately 6 μm and then baked for 2 min at 90 °C. The wafers were subsequently allowed to cool for at least 10 min before exposure.

The resist was exposed to a constant UV dose of 150 mJ/cm^2 and then developed in a mixture of 4:1 H_2O/AK400 (photoresist developer; MicroChemicals GmbH, Ulm, Germany) to completion. After rinsing, the wafers were immediately dried and loaded into an evaporation chamber. After reaching a base pressure of less than 10^{-6} Torr, sequential layers of chromium and gold were deposited with thicknesses of 5 and 175 nm, respectively. After metallization, the wafers were sonicated in acetone to lift off the photoresist, typically requiring approximately 20 min for full lift-off from the substrate. Subsequently, the wafers were rinsed with acetone and further sonicated in successive baths of acetone and isopropanol for 5 min. The wafers were then dried with nitrogen, coated with a protective layer of photoresist and diced into 3 × 1 cm^2 chips. After dicing, the chips were cleaned with acetone and isopropanol and dried with nitrogen. The electrode fingers and the central working area of each chip were then coated with a 1 μm layer of silicon dioxide using plasma enhanced chemical vapor deposition (Plasmalab System 100, Oxford Instruments, Abingdon, U.K.).

The reaction chambers were cast in polydimethylsiloxane (PDMS; Sigma-Aldrich Pty. Ltd., Castle Hill, NSW, Australia) on masters that were fabricated using a 3D printer (Objet Eden 260 V; Stratasys Ltd., Rehovot, Israel). The master consisted of a reaction chamber with a diameter of 8 mm, a height of 2 mm and an approximate volume of 100 μL. The master also had 3 posts with a diameter of 0.5 mm and a height of 2 mm for the inlet and outlet ports. Three pieces of thin silicone tubing (0.02″ ID, 0.05″ OD; Gecko Optical, Joondalup, WA, Australia) were cut to a length of 4 mm and placed on the small posts as fixed inlets and outlet before casting the PDMS (Figure 2). The masters were then placed in a disposable Petri dish and the PDMS, prepared by mixing prepolymer and curing agent in a 10:1 ratio and degassed using a vacuum desiccator, was poured on top to a thickness of approximately 4 mm. The PDMS was then baked at 65 °C for 2 h. Prior to bonding with the PDMS, the lithium niobate substrates were rinsed with acetone and isopropanol, dried with nitrogen and subsequently

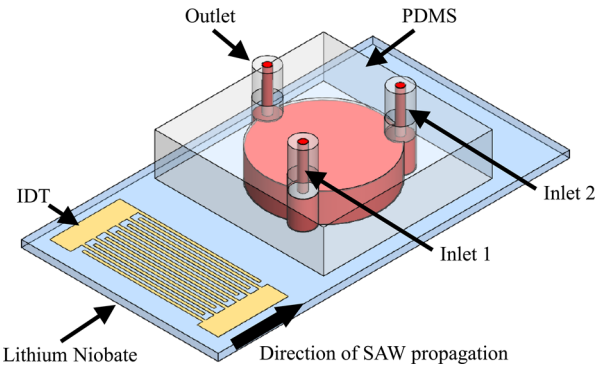

Figure 2. Schematic illustration of the SAW device consisting of the lithium niobate chip on which the IDT is patterned and the PDMS reaction chamber is bonded. The latter comprises two inlet ports for the sample and reagent, and one outlet port. The SAW propagation direction is indicated by the bold arrow; as the SAW comes into contact with the liquid in the chamber, it leaks its energy into the liquid to drive strong chaotic liquid recirculation (i.e., acoustic streaming) within the reaction chamber in order to enhance the mixing within it.

dx.doi.org/10.1021/ac502878p | Anal. Chem. 2014, 86, 10812−10819

exposed to air plasma at a pressure of 400 mTorr for 90 s in a plasma cleaner (Harrick Plasma, Ithaca, NY). Immediately after plasma treatment, the PDMS chambers were pressed into contact with the lithium niobate substrate and then heated in an oven at 60 °C for 1 h to ensure permanent and even bonding. Unless otherwise stated, the inlet and outlet ports are oriented with respect to the IDT as shown in Figure 2.

Device Setup and Characterization. A schematic of the fully assembled device can be seen in Figure 2. These devices were mounted on a custom-made jig that allowed the device to be connected to a signal generator (N9310, Agilent Technologies Pty. Ltd., Mulgrave, VIC, Australia) and amplifier (ZHL-5W-1, Mini-Circuits, Brooklyn, NY, U.S.A.). The operating frequency of the SAW device was fixed at a value between 19.6 and 21.5 MHz, verified for each device using an impedance analyzer (4194A; Agilent Technologies Pty. Ltd., Mulgrave, VIC, Australia). The vibration surface displacement of the device was determined using a high frequency laser Doppler vibrometer (UHF-120-SV; Polytec GmBH, Waldbronn, Germany). All images were taken through the optically transparent, double sided polished lithium niobate substrate.

Samples and reagents were injected into the reaction chamber using syringe pumps (SP100i, World Precision Instruments Inc., Sarasota, FL, U.S.A.) in the qualitative experiments and peristaltic pumps (Ismatec IP-N 4 Channel, IDEX Health & Science GmbH, Wertheim, Germany) in the quantitative experiments. We also verified and demonstrated the possibility for using portable micropumps (M200-P4; RS Compoments Pty. Ltd., Wetherill Park, NSW, Australia) for the purposes of complete integration and miniaturizability of the system, as shown in Figure 1. Syringes were capped with 32 gauge needles (Livingstone International Pty. Ltd., Rosebery, NSW, Australia) threaded onto approximately 50 cm of flexible PVC tubing (0.04″ ID, 0.08″ OD; Ormantine Ltd., Palm Bay, FL, U.S.A.) and microbore PTFE tubing (0.012″ ID, 0.030″ OD; Cole-Parmer Instrument Co., Vernon Hills, IL, U.S.A.), which was subsequently mounted manually onto the input ports of the reaction chamber. The same tubing was also mounted on the outlet end and the waste was dispensed into an amber reagent bottle wrapped in aluminum foil to insulate the detector from any stray chemiluminescent signal arising from further reaction in the waste line. The device was filled with isopropanol and rinsed with water in order to remove air bubbles before operation.

Micromixing Quantification. In order to investigate the effect as well as to optimize the mixing of the chemiluminescent reaction in the continuous flow system, mixtures of 1 mM fluorescein (analytical grade, Sigma-Aldrich Pty. Ltd., Castle Hill, NSW, Australia) and deionized water were initially used. Video images that captured the mixing were then acquired at 50 fps with a high-speed camera (FASTCAM SA-5; Photron Ltd., Tokyo, Japan) ported to an inverted microscope (Eclipse T*i*-S, Nikon Instruments Inc., Tokyo, Japan) with a FITC filter set (Chroma Technology Corp., Bellows Falls, VT, U.S.A.). A 2X objective was used to facilitate full view of the reaction chamber. Images were then cropped to exclude the exterior of the chamber for the purposes of determining the extent of mixing of the reaction in the chamber in each still frame of the video, which is quantified by a mixing index that is defined as follows:[35]

$$\text{mixing index} = \frac{S}{A} \tag{1}$$

wherein S is the image standard deviation, and A the average image intensity. The mixing index was normalized for all SAW experiments such that a mixing index value of unity represents the mixing in the absence of the SAW and a value of zero represents the fully mixed case. Given that the instantaneous normalized mixing indices for each frame stabilized after approximately 20 s, a representative steady-state mixing index for a given parameter set can then be calculated by averaging the instantaneous normalized mixing index over a period ranging from 28 to 30 s.

Chemiluminescent Detection. Initial qualitative chemiluminescent experiments were performed in a darkroom box and recorded with a high resolution camera (EOS 550D SL; Canon Inc., Tokyo, Japan) with a macro lens (EF-S, 60 mm focal length, F2/8; Canon Inc., Tokyo, Japan). The camera was oriented to view the interior of the PDMS reaction chamber from beneath through the transparent lithium niobate substrate. Briefly, 2 mg/L L-proline in pH 9.0 sodium tetraborate buffer was mixed with 0.1 mM $[Ru(bipy)_3]^{3+}$ in 20.0 mM sulfuric acid, whose reaction was given at least 5 min to equilibrate prior to recording for any given flow rate. Once steady-state was reached, a series of images were taken in the darkroom box with an exposure time of 3.2 s keeping the camera setting the same. In order to compare the results of various experiments across a parameter set that allowed a range of flow rates and SAW power inputs to be investigated, the average mixing intensities of the reaction chamber were calculated and normalized against the steady-state mixing intensity in the absence of the SAW input.

Quantitative chemiluminescent detection experiments were carried out by continuously mixing each L-proline standard prepared in 50.0 mM sodium tetraborate buffer at pH 9.0 with the oxidized $[Ru(bipy)_3]^{3+}$ reagent in the interior of the reaction chamber at an optimal combined flow rate of 0.3 mL/min. LabVIEW (National Instruments Corp., Austin, TX, U.S.A.) was used to simultaneously power one set of IDTs by remotely triggering the signal generator to produce directed SAWs at a continuous surface displacement of approximately 1.2 nm. The light signal produced by the chemiluminescent reaction was detected using a PMT (H10721-20; Hamamatsu Photonics K.K., Hamamatsu City, Japan). The photodetector cell was aligned with the reaction chamber (both 8.0 mm in diameter) and the light captured through the lithium niobate wafer at a distance <1 mm; both the reaction chamber and the PMT were isolated in a dark instrument case (ABS Instrument Case with Purge Valve MPV4, Jaycar, Rydalmere, NSW, Australia). The PMT was connected to a data acquisition assistant (NI-USB 6008; National Instruments Corp., Austin, TX, USA) and the data was logged using LabVIEW, which plotted the PMT response (V) against the analysis time (s) as well as the integrated area under each peak (Vs). The chemiluminescent response for each standard was recorded in the form of a baseline acquired over 60 s with the SAW device switched off, followed by a 10 s detection peak obtained with the SAW device switched on. Each standard was analyzed in quintuplicate and a calibration curve was produced for a set of L-proline standards ranging from 0−0.5 ppb.

RESULTS AND DISCUSSION

To enhance the micromixing and hence optimize the chemiluminescent detection, several different parameters were adjusted to investigate their effects on the mixing in the reaction chamber. We first observe in Figure 3 that the mixing

dx.doi.org/10.1021/ac502878p | *Anal. Chem.* 2014, 86, 10812−10819

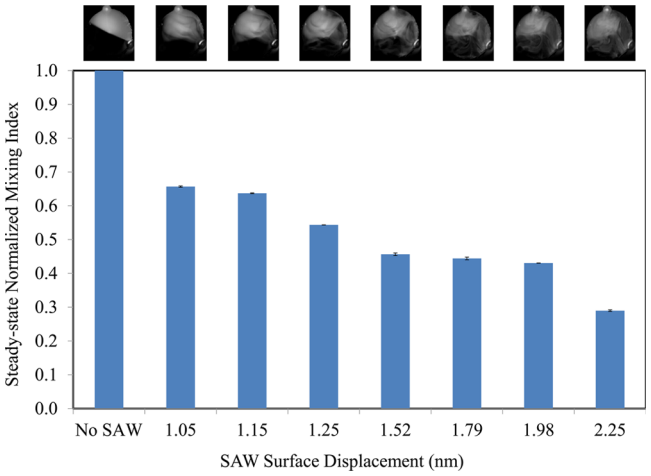

Figure 3. Effect of the SAW surface displacement (which is a function of the SAW input power) on the steady-state normalized mixing index for a combined inlet flow rate of 0.5 mL/min. It can be seen that the mixing is enhanced, reflected by the decrease in the mixing index toward the fully mixed state represented by a null value of the index, with higher surface displacement, i.e., higher power. Also shown above are still images of the reaction chamber captured when at steady-state, showing the mixing (or lack thereof) in the chamber. Each condition was tested once with an average of 100 readings.

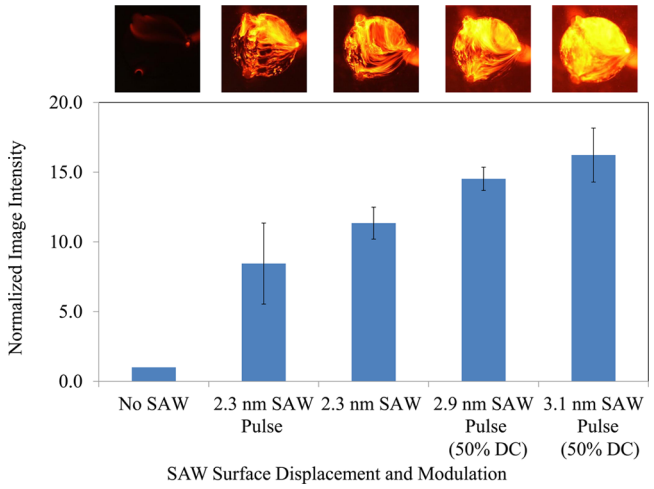

Figure 4. Normalized average pixel intensity for images of the reaction chamber (shown on top) at steady-state as a function of the SAW amplitude and modulation (pulsed operation with 50% duty cycle (DC)) for a combined inlet flow rate of 0.5 mL/min. Error bars indicate 95% confidence intervals. Each condition was tested once, with the normalized average pixel intensity corresponding to the average pixel intensity for the last seven images in a series of ten images given the long exposure time of 3.2 s for each image.

considerably improves when driven actively with the SAW and that the mixing intensity progressively increases with increasing SAW surface displacement (synonymous with the level of the SAW input power), as seen from the decreasing mixing index. This is due to the leakage of the SAW energy into the liquid in the chamber when the SAW comes into contact with the liquid, giving rise to strong liquid recirculation (i.e., acoustic streaming)[28,29] and hence chaotic convection[55] within the reaction chamber such that the laminarity of the flow is disrupted,[56] which leads to a reduction in the diffusion length and time scales, thus resulting in an enhancement in the mixing. Nevertheless, we note that there is a limit to which the SAW surface displacement can be increased, since high input powers beyond 5 W corresponding to a surface displacement amplitude >3.1 nm causes either boiling within the chamber and/or device fracture. To circumvent this limitation, it is possible to cycle the input signal to the SAW on and off rapidly over a pulse period of 500 ms and a pulse width of 250 ms with duty cycles of 25%, 50% and 75%. Using a 50% duty cycle allowed for surface displacements of up to 3.1 nm to be used without adversely affecting the device and further enhancing the mixing, as shown in Figure 4. In addition to improving the mixing efficiency, which can be attributed to intermittency effects which cause further disruption to the flow laminarity,[56] using pulsed in place of the continuous operation has the advantage of reducing power consumption, thus facilitating further possible miniaturization providing the power can be sufficiently reduced such that smaller batteries can be employed; this will be explored in a future study.

Nevertheless, unlike the case of *batch* SAW mixing in sessile drops or closed chambers that have been previously studied,[34−41] there is an additional parameter that has a significant effect on the mixing of the sample and reagent in the system in *continuous flow* devices, namely the liquid flow rate and thus the liquid residence time within the chamber. This effect is shown in Figure 5, wherein it can be generally observed that for a given SAW surface displacement, increases in the

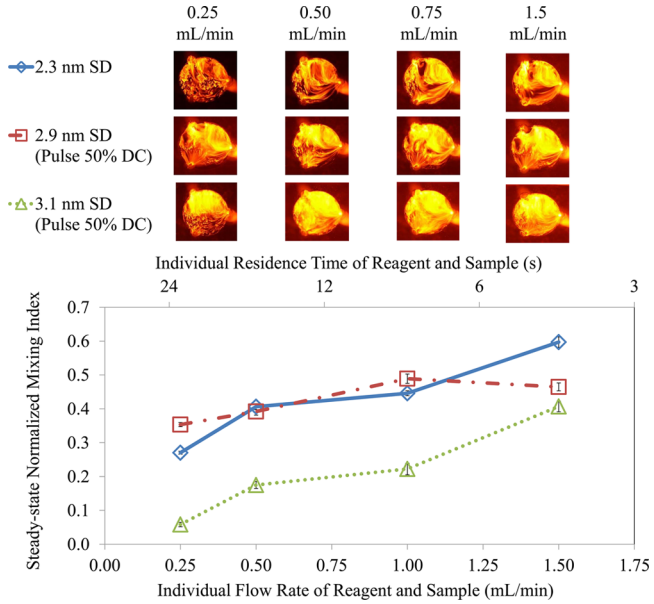

Figure 5. Steady-state normalized mixing index as a function of the volumetric flow rate through the reaction chamber and hence the liquid residence time in the chamber for different SAW surface displacement amplitudes, both in continuous and pulsed (50% duty cycle (DC)) modes. Corresponding images of the chemiluminescent mixing in the reaction chamber are shown above. Error bars represent 95% confidence intervals and the trendlines were added for ease of visualization.

sample and reagent volumetric flow rate to the device causes an increase in the mixing index and hence a deterioration in the mixing intensity. This is because of the decrease in residence time in the reaction chamber, i.e., the duration over which the sample and reagent are exposed to the SAW before they leave the chamber. As such, an increase in the SAW input power is required to maintain the same mixing intensity if the flow rate is increased. Consistent with the results in Figure 4, the mixing

dx.doi.org/10.1021/ac502878p | *Anal. Chem.* 2014, 86, 10812−10819

can be further enhanced for a given flow rate and SAW input power by utilizing the pulsed SAW drive (here, the pulse duty cycle is kept constant at 50%) in place of continuous SAW excitation.

Longer residence times, equating to longer exposure to the SAW, for a fixed volumetric flow rate can also be achieved by varying the orientation of the reaction chamber (i.e., the position of the inlet and outlet ports) with respect to the IDT and hence the SAW propagation direction, as shown in Figure 6. It can clearly be seen that more efficient mixing can be

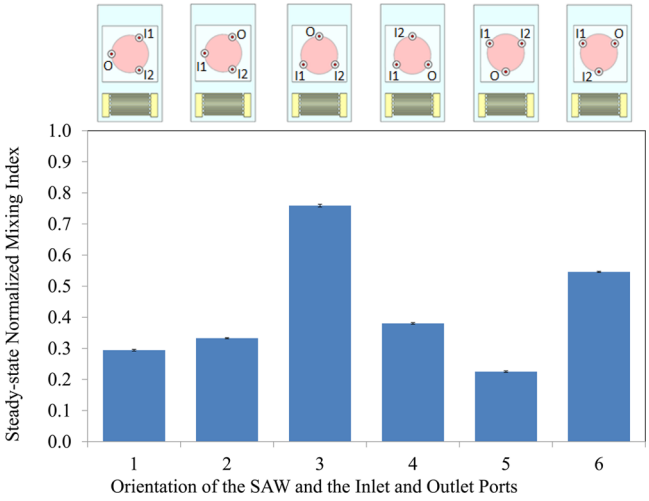

Figure 6. Steady-state normalized mixing index for the different chamber orientations (schematically depicted above the plot), i.e., the position of the inlet (I1 and I2) and outlet (O) ports relative to the IDT and hence the SAW propagation direction. The combined inlet flow rate and the surface displacement was fixed at 0.5 mL/min and 2.5 nm, respectively. Error bars indicate 95% confidence intervals. Each condition was tested once with an average of 100 readings.

obtained when the flow direction is perpendicular to that of the SAW propagation such that the SAW is most efficient in breaking the laminarity of the flow stream from the inlet to the outlet by inducing chaotic convection;[55] similar enhancements in mixing have been reported, for example, when electric fields were applied perpendicular to the laminar flow direction and hence the interface between the streams to be mixed.[57] Nevertheless, we note that the mixing can be further improved, however, by orienting the flow direction counter to that of the SAW propagation (i.e., configuration 5), for example, by positioning the inlet ports on the far side directly opposite the IDT and the outlet port on the near side of the IDT. This observation confirms that the mixing enhancement in our system is not solely due to the introduction of chaotic convection to disrupt the laminarity of the flow but also due to the increased residence time of the liquid in the reaction chamber, and hence the time over which the liquid is exposed to the SAW irradiation.

Figure 7 shows the detection of proline with $[Ru(bipy)_3]^{3+}$ using the PMT that was integrated into the chip-scale platform for the concentrations analyzed, i.e., 0−0.5 ppb. We note that the chemiluminescent signal produced by the mixing inside the reaction chamber varies randomly about the mean intensity. For such processes, the limit of detection can be calculated as three times the experimental standard deviation of the mean of the blank readings σ, divided by the slope of the calibration curve m, i.e., LOD = $3\sigma/m$;[17,58] we note σ is a function of the

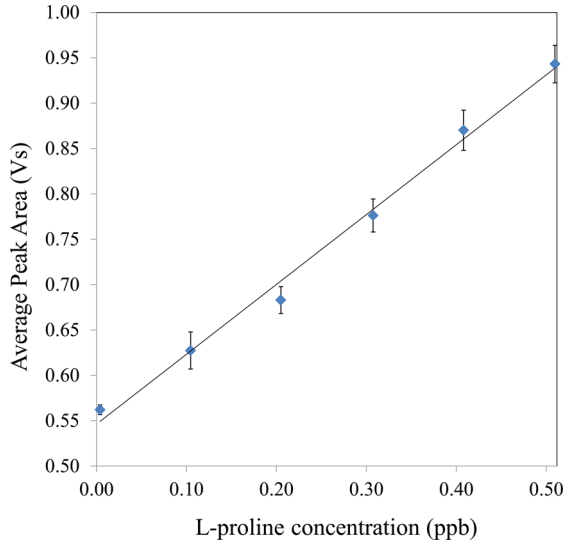

Figure 7. Detection of proline using the PMT integrated into the continuous flow microfluidic device in the presence of SAW micromixing (1.2 nm surface displacement in the absence of pulsing and a combined inlet flow rate of 0.3 mL/min). The slope was obtained by linear regression with R^2 = 0.9929. Error bars indicate experimental standard deviation of the mean.

uncertainty in the chemiluminescent signal, i.e., $\sigma(\bar{q}) = \sigma q_k/\sqrt{n}$, in which $\bar{q}$ represents the arithmetic mean of n independent repeated observations q_k.[59] From this calculation, we calculate the LOD for L-proline to be 0.02 ppb with active micromixing driven by the SAW, thus achieving a detection limit that is two orders of magnitude more sensitive than that obtained with conventional benchscale FIA instrumentation for the same reaction[25] and an order of magnitude more sensitive than the industry gold standard value for the detection of water pollutants found at sub-ppb levels in source waters.[9]

CONCLUSIONS

A portable and lightweight microfluidic flow injection analysis platform which integrates a SAW device into a continuous flow system fitted with a miniaturized photodetection scheme for the microanalytical quantification of chemiluminescent species in the liquid phase is reported. We show that coupling acoustic energy into the liquid flowing through a microfabricated reaction chamber cast in PDMS and bonded onto the SAW chip drives strong and chaotic acoustic streaming that disrupts the laminarity of the flow, significantly enhancing the mixing within the chamber and thus allowing rapid in-line detection of the chemiluminescent signal emitted by the reaction.

In particular, we demonstrate that it is possible to achieve hundredfold improvement in the detection limit to ng/L or parts per trillion sensitivity with the device compared to the limits of detection reported for conventional flow injection analysis systems, but without necessitating sample preconcentration—a severe limitation that has hampered other attempts to miniaturize flow injection systems. The low cost and small size of the system further facilitates high throughput operation through scale out (i.e., numbering up as opposed to scaling up) of the system via the adoption of a large number of devices in parallel; a significant advantage of such scaling out is the ease in replacing a single device in the event of a fault or when maintenance is required without necessitating complete shutdown of an entire operation. This on-chip microfluidic

dx.doi.org/10.1021/ac502878p | Anal. Chem. 2014, 86, 10812−10819

mixing strategy, together with the integrated miniature photodetector and chip-scale microfluidic actuation using the same SAW setup, then suggests that a completely miniaturized low cost and lightweight platform that is sufficiently sensitive as a portable field-use microanalytical system is within reach.

AUTHOR INFORMATION

Corresponding Author

*E-mail: leslie.yeo@rmit.edu.au.

Notes

The authors declare no competing financial interest.

ACKNOWLEDGMENTS

This work was in part supported by ARC Discovery grants DP1092955 and DP120100013. A.M.G.M. is a recipient of funding from Water Research Australia (WATERRA). L.Y.Y. also acknowledges funding through an Australian Research Council Future Fellowship (FT130100672), whereas J.R.F. is grateful to RMIT University for a Vice-Chancellor's Senior Research Fellowship.

REFERENCES

(1) Nacapricha, D.; Sastranurak, P.; Mantim, T.; Amornthammarong, N.; Uraisin, K.; Boonpanaid, C.; Chuyprasartwattana, C.; Wilairat, P. *Talanta* **2013**, *110*, 89−95.

(2) van Staden, J. F.; van Staden, R. I. S. *Talanta* **2012**, *102*, 34−43.

(3) Miró, M.; Cerdà, V.; Estela, J. M. *TrAC, Trends Anal. Chem.* **2002**, *21*, 199−210.

(4) Ranger, C. B. *Anal. Chem.* **1981**, *53*, 20A−32A.

(5) Betteridge, D. *Anal. Chem.* **1978**, *50*, 832A−846A.

(6) Worsfold, P. J.; Clough, R.; Lohan, M. C.; Monbet, P.; Ellis, P. S.; Quétel, C. R.; Floor, G. H.; McKelvie, I. D. *Anal. Chim. Acta* **2013**, *803*, 15−40.

(7) Dănet, A.; Cheregi, M.; Calatayud, J. M.; Mateo, J. V. G.; Enein, H. Y.A. *Crit. Rev. Anal. Chem.* **2001**, *31*, 191−222.

(8) Lyddy-Meaney, A. J.; Ellis, P. S.; Worsfold, P. J.; Butler, E. C.; McKelvie, I. D. *Talanta* **2002**, *58*, 1043−1053.

(9) *National Water Quality Management Strategy−Australian Drinking Water Guidelines Paper 6*, National Health & Medical Research Council and National Resource Management Ministerial Council, Commonwealth of Australia, Canberra, 2011.

(10) Wilson, R.; Barker, M. H.; Schiffrin, D. J.; Abuknesha, R. *Biosens. Bioelectron.* **1997**, *12*, 277−286.

(11) Galeano Díaz, T.; Acedo Valenzuela, M.; Salinas, F. *Anal. Chim. Acta* **1999**, *384*, 185−191.

(12) Vílchez, J.; Valencia, M.; Navalón, A.; Molinero-Morales, B.; Capitán-Vallvey, L. *Anal. Chim. Acta* **2001**, *439*, 299−305.

(13) Li, Y.; Yang, F.; Yang, X. *Analyst* **2009**, *134*, 2100−2105.

(14) Jain, S.; Borowska, E.; Davidsson, R.; Tudorache, M.; Pontén, E.; Emnéus, J. *Biosens. Bioelectron.* **2004**, *19*, 795−803.

(15) Pérez-Ruiz, T.; Martinez-Lozano, C.; Sanz, A.; Val, O. *Anal. Chim. Acta* **1993**, *284*, 173−179.

(16) Súbová, I.; Khenlami Assandas, A.; Catalá Icardo, M.; Martínez Calatayud, J. *Anal. Sci.* **2006**, *22*, 21−24.

(17) Gómez-Benito, C.; Meseguer-Lloret, S.; Torres-Cartas, S. *Int. J. Environ. Anal. Chem.* **2013**, *93*, 152−165.

(18) Gámiz-Gracia, L.; García-Campaña, A. M.; Soto-Chinchilla, J. J.; Huertas-Pérez, J. F.; González-Casado, A. *TrAC, Trends Anal. Chem.* **2005**, *24*, 927−942.

(19) Gámiz-Gracia, L.; García-Campaña, A. M.; Huertas-Pérez, J. F.; Lara, F. J. *Anal. Chim. Acta* **2009**, *640*, 7−28.

(20) Mirasoli, M.; Guardigli, M.; Michelini, E.; Roda, A. *J. Pharm. Biomed. Anal.* **2014**, *87*, 36−52.

(21) Mansur, E. A.; Ye, M.; Wang, Y.; Dai, Y. *Chin. J. Chem. Eng.* **2008**, *16*, 503−516.

(22) Terry, J. M.; Adcock, J. L.; Olson, D. C.; Wolcott, D. K.; Schwanger, C.; Hill, L. A.; Barnett, N. W.; Francis, P. S. *Anal. Chem.* **2008**, *80*, 9817−9821.

(23) Terry, J. M.; Zammit, E. M.; Slezak, T.; Barnett, N. W.; Olson, D. C.; Wolcott, D. K.; Edwards, D. L.; Francis, P. S. *Analyst* **2011**, *136*, 913−919.

(24) Terry, J. M.; Mohr, S.; Fielden, P. R.; Goddard, N. J.; Barnett, N. W.; Olson, D. C.; Wolcott, D. K.; Francis, P. S. *Anal. Bioanal. Chem.* **2012**, *403*, 2353−2360.

(25) Costin, J. W.; Barnett, N. W.; Lewis, S. W. *Talanta* **2004**, *64*, 894−898.

(26) He, L.; Cox, K. A.; Danielson, N. D. *Anal. Lett.* **1990**, *23*, 195−210.

(27) Jackson, W. A.; Bobbitt, D. R. *Anal. Chim. Acta* **1994**, *285*, 309−320.

(28) Yeo, L. Y.; Friend, J. R. *Biomicrofluidics* **2009**, *3*, 012002.

(29) Friend, J.; Yeo, L. Y. *Rev. Mod. Phys.* **2011**, *83*, 647.

(30) Ding, X.; Li, P.; Lin, S.-C. S.; Stratton, Z. S.; Nama, N.; Guo, F.; Slotcavage, D.; Mao, X.; Shi, J.; Costanzo, F.; Huang, T. J. *Lab Chip* **2013**, *13*, 3626−3649.

(31) Yeo, L. Y.; Friend, J. R. *Annu. Rev. Fluid Mech.* **2014**, *46*, 379−406.

(32) Frommelt, T.; Kostur, M.; Wenzel-Schäfer, M.; Talkner, P.; Hänggi, P.; Wixforth, A. *Phys. Rev. Lett.* **2008**, *100*, 034502.

(33) Shilton, R. J.; Yeo, L. Y.; Friend, J. R. *Sens. Actuators, B* **2011**, *160*, 1565−1572.

(34) Sritharan, K.; Strobl, C.; Schneider, M.; Wixforth, A.; Guttenberg, Z. v. *Appl. Phys. Lett.* **2006**, *88*, 054102.

(35) Li, H.; Friend, J. R.; Yeo, L. Y. *Biomed. Microdevices* **2007**, *9*, 647−656.

(36) Renaudin, A.; Chabot, V.; Grondin, E.; Aimez, V.; Charette, P. G. *Lab Chip* **2010**, *10*, 111−115.

(37) Alghane, M.; Chen, B.; Fu, Y.; Li, Y.; Luo, J.; Walton, A. *J. Micromech. Microeng.* **2011**, *21*, 015005.

(38) Ducloux, O.; Galopin, E.; Zoueshtiagh, F.; Merlen, A.; Thomy, V. *Biomicrofluidics* **2010**, *4*, 011102.

(39) Li, Y.; Fu, Y.; Brodie, S.; Alghane, M.; Walton, A. *Biomicrofluidics* **2012**, *6*, 012812.

(40) Tseng, W.-K.; Lin, J.-L.; Sung, W.-C.; Chen, S.-H.; Lee, G.-B. *J. Micromech. Microeng.* **2006**, *16*, 539−548.

(41) Shilton, R.; Tan, M. K.; Yeo, L. Y.; Friend, J. R. *J. Appl. Phys.* **2008**, *104*, 014910.

(42) Tan, M.; Yeo, L.; Friend, J. *EPL (Europhys. Lett.)* **2009**, *87*, 47003.

(43) Glass, N.; Shilton, R.; Chan, P.; Friend, J.; Yeo, Y. *Small* **2012**, *8*, 1881−1888.

(44) Rezk, A. R.; Qi, A.; Friend, J. R.; Li, W. H.; Yeo, L. Y. *Lab Chip* **2012**, *12*, 773−779.

(45) Dentry, M. B.; Friend, J. R.; Yeo, L. Y. *Lab Chip* **2014**, *14*, 750−758.

(46) Gerardi, R.; Barnett, N.; Lewis, S. *Anal. Chim. Acta* **1999**, *378*, 1−41.

(47) Brune, S. N.; Bobbitt, D. R. *Anal. Chem.* **1992**, *64*, 166−170.

(48) Bobbitt, D. R.; Jackson, W. A.; Hendrickson, H. P. *Talanta* **1998**, *46*, 565−572.

(49) Costin, J. W.; Francis, P. S.; Lewis, S. W. *Anal. Chim. Acta* **2003**, *480*, 67−77.

(50) Gorman, B. A.; Francis, P. S.; Barnett, N. W. *Analyst* **2006**, *131*, 616−639.

(51) Hosono, H.; Satoh, W.; Fukuda, J.; Suzuki, H. *Sens. Actuators, B* **2007**, *122*, 542−548.

(52) Damrauer, N. H.; Cerullo, G.; Yeh, A.; Boussie, T. R.; Shank, C. V.; McCusker, J. K. *Science* **1997**, *275*, 54−57.

(53) Lee, W.; Nieman, T. *Anal. Chem.* **1995**, *67*, 1789−1796.

(54) Adcock, J. L.; Francis, P. S.; Barnett, N. W. *Anal. Chim. Acta* **2007**, *601*, 36−67.

(55) Shilton, R.; Yeo, L.; Friend, J. *Sens. Actuators, B* **2011**, *160*, 1565−1572.

(56) Ottino, J. *Annu. Rev. Fluid Mech.* **1990**, *22*, 207−254.

(57) Lin, H.; Storey, B. D.; Oddy, M. H.; Chen, C.-H.; Santiago, J. G. *Phys. Fluids* **2004**, *16*, 1922−1935.
(58) Fonollosa, J.; Vergara, A.; Huerta, R.; Marco, S. *Anal. Chim. Acta* **2014**, *810*, 1−9.
(59) JCGM 100:2008 *Evaluation of Measurement Data—Guide for the Expression of Uncertainty in Measurement*, (Joint Committee for Guides in Metrology: Bureau International des Poids et Mesures BIPM, International Electrotechnical Commission IEC, International Federation of Clinical Chemistry & Laboratory Medicine IFCC, International Laboratory Accreditation Cooperation ILAC, International Standards Organization ISO, International Union of Pure & Applied Chemistry IUPAC, International Union of Pure & Applied Physics IUPAP, Organisation Internationale de Métrologie Légale OIML) 2008.